ARTICLE
Traditional Medicine Research 2023;8(1):4. https://doi.org/10.53388/TMR20220608001

Oriental Medicine

Rutaecarpine attenuates monocrotaline-induced pulmonary arterial hypertension in a Sprague-Dawley rat model

Xiao-Wei Gong[1], Yan-Ling Sheng[2], Shi-Wei Kang[1], Bo-Yun Yuan[1], Ya-Dong Yuan[1*]

[1]Department of Respiratory and Critical Care Medicine, The Second Hospital of Hebei Medical University, Shijiazhuang 050000, China. [2]Department of Respiratory and Critical Care Medicine, Huabei Petroleum Administration Bureau General Hospital, Renqiu 062550, China.

[*]**Corresponding to:** Ya-Dong Yuan, Department of Respiratory and Critical Care Medicine, The Second Hospital of Hebei Medical University, No. 215, Heping West Road, Shijiazhuang 050073, China. E-mail: yuanyd1108@163.com.

Author contributions

Xiao-Wei Gong and Ya-Dong Yuan designed the experiment, Xiao-Wei Gong, Yan-Ling Sheng, Shi-Wei Kang, Bo-Yun Yuan were responsible for experimental implementation, Xiao-Wei Gong and Shi-wei Kang were responsible for data collation, Xiao-Wei Gong was responsible for paper writing and Ya-Dong Yuan was responsible for manuscript review. All authors have read and approved the final version of this manuscript.

Competing interests

The authors declare no conflicts of interest.

Acknowledgments

This work was supported by Hebei Provincial Government Funded Clinical Medicine Excellent Talents Training Team Project (2020), Scientific Research Project of Hebei Administration of Traditional Chinese Medicine (2016045). We thank Inovelt Ltd. for editing the English text of a draft of this manuscript.

Abbreviations

PAH, pulmonary arterial hypertension; PAEC, pulmonary artery endothelial cell; PASMC, pulmonary artery smooth muscle cell; MCT, monocrotaline; α-SMA, alpha-smooth muscle actin; PCR, polymerase chain reaction; Bax, Bcl-2-associated X; TNF-α, tumor necrosis factor-α; IL-6, interleukin-6; IL-1β, interleukin-1β; NF-κB, nuclear factor kappa-B; ET-1, endothelin-1; p-ERK1/2, phospho-extracellular signal-regulated kinases 1/2; Bcl-2, B cell lymphoma-2; LC3, microtubule- associated protein light chain 3; SOD, superoxide dismutase; MDA, malondialdehyde; GSH-Px, glutathione peroxidase; mPAP, mean pulmonary artery pressure; RV, right ventricle; LV, left ventricle; CW, cardiac weight; BW, body weight; %MWT, percentage of medial wall thickness; RT-qPCR, reverse transcription-quantitative PCR; H&E, hematoxylin-eosin; MAPK, mitogen-activated protein kinase.

Peer review information

Traditional Medicine Research thanks all anonymous reviewers for their contribution to the peer review of this paper.

Citation

Gong XW, Sheng YL, Kang SW, Yuan BY, Yuan YD. Rutaecarpine attenuates monocrotaline-induced pulmonary arterial hypertension in a Sprague-Dawley rat model. *Tradit Med Res*. 2023;8(1):4. doi: 10.53388/TMR20220608001.

Executive editor: Guang-Ze Ma.

Received: 08 June 2022; **Accepted:** 07 July 2022; **Available online:** 20 July 2022.

Abstract

Background: Pulmonary arterial hypertension presents with obliterative remodeling of the pulmonary arteries and progressive elevation of pulmonary vascular resistance, which increase the risk of right ventricular failure and death. It has been reported in previous studies that rutaecarpine plays a crucial role in anti-inflammatory and antioxidant activities, which may help regulate cell apoptosis and cell proliferation. The purpose of this study was to determine the effects of rutaecarpine in the rat model of monocrotaline-induced pulmonary hypertension. **Methods:** We induced pulmonary arterial hypertension in adult Sprague-Dawley rats by injecting monocrotaline (60 mg/kg) and then treated with rutaecarpine (40 mg/kg·d) or sildenafil (30 mg/kg·d) (positive control). Subsequently, pulmonary function, inflammation, cytokines and pulmonary vascular remodeling or proliferation were assessed. **Results:** Rutaecarpine was found to improve monocrotaline-induced mean pulmonary artery pressure, cardiac index, right heart index, right ventricular hypertrophy index, pulmonary artery remodeling and pulmonary function. reverse transcription- quantitative polymerase chain reaction demonstrated a decrease in tumor necrosis factor-α, interleukin-6 and interleukin-1β, whereas western blots a significantly decrease in the expression of nuclear factor kappa-B, endothelin-1, extracellular signal-regulated kinases 1/2, B cell lymphoma-2, Beclin1 and microtubule-associated protein1 light chain 3-II protein, and increase in the expression of Bax, caspase-3 and p62 protein. **Conclusion:** Rutaecarpine attenuated pulmonary arterial hypertension by inhibiting inflammation, oxidative stress, cell proliferation and autophagy, while promoting apoptosis.

Keywords: rutaecarpine; pulmonary arterial hypertension; inflammatory response; oxidative stress; vascular proliferation

Highlights

This study was the first to comprehensively explore the mechanism of rutaecarpine, the main active component of *Evodia rutaecarpa*, in pulmonary hypertension induced by monocrotaline. This study found that rutaecarpine can reverse monocrotaline-pulmonary arterial hypertension by inhibiting inflammation, oxidative stress, cell proliferation and autophagy, while promoting apoptosis. The effect of rutaecarpine on pulmonary arterial hypertension is similar to that of sildenafil.

Medical history of objective

Evodia rutaecarpa, a traditional Chinese medicine, was first recorded in *Shennong's Classic of Materia Medica* (Unknow author, 25–220 C.E.). It has been used in clinical settings in Asia for more than 1,000 years. Its pharmacological effect is extensive and has broad research value. It has the effect of warming meridians, dispelling cold, lowering adverse Qi (In traditional Chinese medicine, it refers to the most fundamental and subtle substances that constitute the human body and maintain life activities. At the same time, it also has the meaning of physiological function. In terms of traditional Chinese medicine, Qi and different words are used together to express different meanings), stop vomiting, etc., and widely used to treat cardiovascular and cerebrovascular diseases, digestive system diseases, endocrine system diseases, gynecological diseases, skin diseases and so on. Rutaecarpine is one of *Evodia rutaecarpa*'s main active components. Multiple in vitro studies have already reported that rutaecarpine exerts a positive inotropic effect in the heart, promotes vasodilation and consequently lowers blood pressure, exhibits protective effects against gastric mucosal damage and ulcerative proctitis, as well as anti-inflammatory, antitumor, antiviral, analgesic effects.

Background

The disease of pulmonary arterial hypertension (PAH) is known for its progression and poor prognosis and it ultimately leads to right heart failure and death as a consequence of right heart failure [1]. At present, the 5-year survival rate of PAH is only 57%, although targeted therapies are conducted [2]. PAH treatment relies on the administration of approved drugs focused on the vasoconstrictive phenotype of the disease and its benefits are restricted [3]. Therefore, new therapeutic agents should be developed to improve the pulmonary vascular remodeling process.

According to previous studies, the major mechanism of pulmonary vascular resistance is pulmonary artery endothelial cell (PAEC) dysfunction, as well as pulmonary artery smooth muscle cell (PASMC) proliferation, hypertrophy and collagen accumulation [4]. Hypoxia of pulmonary artery endothelium results in the production and release of inflammatory cytokines, which may cause abnormal proliferation of PASMCs, vasoconstriction and vascular remodeling [5]. Furthermore, the inflammatory cytokines may affect pulmonary vascular remodeling and this feature plays a role in the progression of PAH through modulation of the proliferation and migration of pulmonary vascular cells [6–8]. Additionally, hyperproliferation and apoptosis-resistant PASMCs could thicken pulmonary vessel walls and remodel the vasculature [9]. Therefore, treatment strategies for PAH should include attenuation of PAEC dysfunction, inhibition of inflammation and reduction of the abnormal proliferation of PASMCs.

Evodia rutaecarpa is a traditional Chinese medicine. It was the first recorded in *Shennong's Classic of Materia Medica* and has been used to treat cardiovascular and cerebrovascular diseases, digestive system diseases, endocrine system diseases, gynecological diseases, skin diseases and so on for more than 1,000 years. Rutaecarpine, an indolequinazoline alkaloid, is a major active component in *Evodia rutaecarpa* [10]. Its pharmacological effect is extensive and has broad research value. Studies have already reported that rutaecarpine act as a protective agent in colitis, atherosclerosis, Alzheimer's disease, cerebral ischemia-reperfusion injury and hypoxia-related right heart remodeling [11–15]. Rutaecarpine exerts anti-oxidative, anti-inflammatory and pro-apoptotic properties through the nuclear factor kappa-B (NF-κB), nuclear factor erythroid-2 related factor 2/heme oxygenase-1 and B cell lymphoma-2 (Bcl-2)/Bcl-2-associated X (Bax) pathways [16–18]. Therefore, our study investigated the effects of rutaecarpine in the monocrotaline (MCT) rat model of PAH.

Materials and Methods

Chemicals, reagents and antibodies

Rutaecarpine was purchased from Shanghai Yuanye Biological Technology Co., Ltd. ($C_{18}H_{13}N_3O$; molecular weight, 287.32 Da; Shanghai, China). MCT was purchased from Sigma (St. Louis, MO, USA). Sildenafil was purchased from Pfizer Biopharmaceutical Co., Ltd. (New York, NY, USA). Total DNA and RNA extraction kits, polymerase chain reaction (PCR) kit, first-stand cDNA reverse transcription kits and primers were all from Tiangen Biotechnology Co., Ltd. (Beijing, China). Bax (14796), caspase-3 (9662), phospho-extracellular signal-regulated kinases 1/2 (p-ERK1/2) (4370), t-ERK1/2 (4695), and NF-κB p65 (8242) were purchased from Cell Signaling Technology, Inc. (Boston, MA, USA); microtubule-associated protein light chain 3 (LC3) (14600-1-AP), Beclin1 (11306-1-AP), p62 (18420-1-AP) and β-actin (20536-1-AP) were purchased from Proteintech Group, Inc. (Wuhan, China). alpha-smooth muscle actin (α-SMA) (ab7817) , Bcl-2 (ab194583) and endothelin-1 (ET-1) (ab2786) were all from Abcam (Shanghai, China). Nanjing Jiancheng Biological Engineering Institute (Nanjing, China) provided superoxide dismutase (SOD), malondialdehyde (MDA) and glutathione peroxidase (GSH-Px) test kits.

Animal experiments

Beijing Huafukang Biological Technology Co., Ltd. (Beijing, China, approval number: IRM-DWLL-2020092) provided Sprague-Dawley male rats (6–8 weeks, 200 ± 20 g) . Animal experiments were approved by the Second Hospital of Hebei Medical University's Committee on Laboratory Animal Care and Use (ethics number: 2015-R142). All animal care and experiments complied with the Animal Research: Reporting of In Vivo Experiments (ARRIVE) guidelines and were performed in accordance with the guidelines prescribed by the Guide for the Care and Use of Laboratory Animals of the Second Hospital of Hebei Medical University Animal Experiment Centre. All rats were housed in the same room with provision of a standard diet and water ad libitum in an environment of 20 ± 2 °C and a 12-h light/dark cycle. Four groups, each with 12 mice, were randomly assigned control group, MCT group, rutaecarpine group (MCT + Rut) and sildenafil group (MCT + Sil). Starting from the day of MCT injection (60 mg/kg), rats in the rutaecarpine group were given rutaecarpine intragastric administration (40 mg/kg·d) [19, 20]. The positive control group was treated with sildenafil intragastric administration (30 mg/kg·d) [21]. Matching placebo (normal saline) administered in the same manner between the control and the model group. This study lasted for four weeks.

Lung function test, hemodynamic experiments and morphological investigation

Lung function was measured using a Buxco small animal lung function detection system (America) according to manufacturer's instructions. To measure the mean pulmonary artery pressure (mPAP), we inserted a polyethene catheter (PE-50 Intramedic PE tubing; Becton Dickinson, Franklin Lakes, NJ, USA) from the right external jugular vein and advanced into the pulmonary artery of the anesthetized rats [22]. Then used the PowerLab system connected to a pressure transducer (AD Instruments, Colorado Springs, CO, USA) to record the data. After the conduction of hemodynamic measurements, we anesthetized rats with intraperitoneal injections of 3% sodium pentobarbital (45 mg/kg), then killed by bloodletting after carotid blood sampling, and the lung and heart specimens were collected for histological evaluation. Wet weights of the right ventricle (RV) and left ventricle

(LV) + interventricular septum (S) were used to estimate the RV hypertrophy index, calculated by using (RV/(LV + S)). The cardiac weight (CW) and body weight (BW, measured before dissection) were used to evaluate the cardiac index, calculated by using (CW/BW). RV index obtained using wet RV weight (RVW)/wet BW.

Immunohistochemical staining

A hematoxylin and eosin (H&E) stain stain was used to demonstrate pulmonary vascular remodeling. We fixes the right lung lobe and RV tissues in 10% formaldehyde for 48 h and then washed with distilled water for 10 min. Ethanol was then used to dehydrate the samples in a stepwise manner, embedded in wax and sectioned. In the following steps, we used H&E or Masson's trichrome to stain the sections. Additionally, calculating percentage of medial wall thickness (%MWT) as ((external diameter − internal diameter)/external diameter) × 100% to estimate pulmonary vascular remodeling [23]. The level of pulmonary arterial modification was evaluated by performing α-SMA immunohistochemical staining [24]. The paraffin-embedded blocks were sectioned into continuous sections (4 μm) and mounted onto silane-coated slides. We rehydrated the dewaxed lung tissue sections, then washed them with phosphate buffer saline (pH 7.2–7.4). After conducting blocking with 5% bovine serum albumin, the sections were incubated overnight at 4 ˚C with α-SMA monoclonal antibodies (1:500), followed by incubation with the horseradish peroxidase-conjugated secondary antibodies (1:200). Light microscopy was used to evaluate all the stained sections (400× magnification; Nikon, Japan). In each group, five fields from six sections were randomly selected for representation.

Western blot analysis

The levels of ERK1/2, p-ERK1/2, NF-κB p65, ET-1, Bcl-2, Bax, pro-caspase-3, cleaved caspase-3, p62, Beclin1, LC3 were detected by Western blot analysis. We extracted proteins from lung tissue following standard protocols and we measure protein levels using bicinchoninic acid assay. After electrophoresis, the protein was transferred to polyvinylidene fluoride membrane, sealed with 5% dry skim milk at room temperature for 1 h and then incubated at 4 ˚C overnight in the primary antibody solution. The following day, the membrane was then incubated for 2 hour with horseradish peroxidase-conjugated second antibody at room temperature. After washing three times with washing buffer, reactivity was detected and visualized using the enhanced chemiluminescence Bio-Spectrum gel imaging system (UVP, Upland, CA, USA). mRNA expression was measured against β-actin.

Reverse transcription-quantitative PCR (RT-qPCR)

We used RT-qPCR to measure mRNA levels of tumor necrosis factor-α (TNF-α), interleukin-6 (IL-6) and interleukin-1β (IL-1β) [25]. According to the instructions, total RNA was extracted using plant RNA extraction kit (TransGen Biotech, Beijing, China). The PrimerScript RT reagent kit (Takara, Shiga, Japan) was used to reverse transcript the RNA. We used the SYBR Green RT-qPCR SuperMix kit (Thermo Fisher Scientific, Waltham, MA, USA) with customized primers (Table 1) using the AB7300 thermo-cycler (Applied Biosystems, Foster, CA, USA) to perform real-time PCR analysis on quantify relative RNA levels. Internal controls were performed using β-actin. We calculated relative expression level using $2^{-\Delta\Delta Ct}$ method.

Oxidative stress

The SOD level was measured using a superoxide assay kit (Beyotime Biotech Inc., Shanghai, China), whereas MDA level was measured using a lipid peroxidation MDA assay kit (Beyotime Biotech Inc., Shanghai, China). GSH-Px was measured using a GSH-Px assay kit (Beyotime Biotech Inc., Shanghai, China) [26]. All operations were conducted in accordance with the manufacturer's instructions.

Statistical analysis

We present all our data as mean ± standard deviation. Group comparisons were performed using one-way analysis of variance followed by Tukey's post hoc test. *P*-values reported in this study are two-sided and $P < 0.05$ is considered statistically significant. We used solutions statistical package for the social sciences statistical software (version 22. 0, SPSS Inc., Chicago, IL, USA) for statistical analysis.

Results

General rat characteristics

When compared with the normal control group, BW growth was significantly retarded in the three MCT groups ($P < 0.01$). Moreover, significant changes in pulmonary function were observed in MCT rats, and such changes mainly manifested as decreased lung compliance and increased inspiratory resistance; these aspects were significantly improved following rutaecarpine and sildenafil treatment ($P < 0.05$) (Table 2).

Rutaecarpine attenuates hemodynamics, right ventricular hypertrophy and vascular remodeling

The hemodynamic changes were monitored and results revealed that MCT-treated rats displayed significantly higher mPAP than the control group ($P < 0.01$), whereas this effect was diminished by rutaecarpine 1A), right heart index (Figure 1B) and right heart hypertrophy index and sildenafil ($P < 0.01$) (Table 2). Compared to the control group, MCT-treated rats showed a significantly increased heart index (Figure 1A), right heart index (Figure 1B), and right heart hypertrophy index (Figure 1C) 4 weeks after subjection to a single intraperitoneal

Table 1 Experimental design

	Number (n)	Treatment
Group 1 (Control group)	12	Received saline injection intraperitoneally (i.p.) on day 1 and then with an equal volume of vehicle (0.9% NaCl) alone for 28 days
Group 2 (MCT group)	12	Received a single intraperitoneally injection of MCT (60 mg/kg) at day 1, pulmonary hypertension model was established for 28 days [23]
Group 3 (MCT + Rut group)	12	Received rutaecarpine (40 mg/kg) by daily gavage tube for 28 days after MCT injection [24]
Group 4 (MCT + Sil group)	12	Received sildenafil (25 mg/kg) by daily gavage tube for 28 days after MCT injection [25]

MCT, monocrotaline.

Table 2 Primary antibody for western blot

Primary antibody	Concentration	Primary antibody	Concentration
Bcl-2	1:1,000	p65	1:1,000
Bax	1:2,000	LC3	1:1,000
Caspase-3	1:1,000	Beclin1	1:2,000
p-ERK1/2	1:2,000	p62	1:2,000
t-ERK1/2	1:1,000	β-Actin	1:10,000
ET-1	1:500		

Bcl-2, B cell lymphoma-2; Bax, Bcl-2-associated X; p-ERK1/2, phospho-extracellular signal-regulated kinases 1/2; t-ERK1/2, total-extracellular signal-regulated kinases 1/2; ET-1, endothelin-1; LC3, microtubule- associated protein light chain 3.

injection. However, following intragastric administration of rutaecarpine, the heart index, right heart index and right heart hypertrophy index significantly decreased. Similarly, the MCT + Sil group showed a significantly improved right heart hypertrophy index, but without exhibition of significant improvements in heart index and right heart index.

Pathological changes of small and medium pulmonary arteries (50–200 μm) were observed via H&E (Figure 2A) and Masson's trichrome staining (Figure 2B) procedures. In the control group, the pulmonary artery wall was observed to be thin, with a normal lumen and without inflammatory cell infiltration. In contrast, in MCT-treated rats, the wall of the pulmonary arterioles was significantly thickened, additionally, we observed a large number of inflammatory cells around the blood vessels and surrounding tissues. Smooth muscle cells indicated significant proliferation and were arranged in a disorderly manner with a narrow lumen. The vascular morphology of rats in the MCT + Rut group was significantly improved, similar to that observed in the MCT + Sil group. A quantitative analysis showed that the %MWT (Figure 2D) of pulmonary arterioles in rats treated with MCT increased 3.42-fold, compared to the control group ($P < 0.01$). In contrast, sildenafil and rutaecarpine treatment successfully reversed the %MWT of MCT-induced pulmonary arterioles ($P < 0.01$).

The Masson's trichrome staining results demonstrated that there were few collagen fibers and inflammatory cells present in untreated control rats. In the MCT group, a considerable number of disordered and proliferated collagen fibers were present, along with numerous inflammatory cells in the vascular wall and surrounding tissues. Collagen fiber proliferation and inflammatory cell infiltration in the MCT + Rut group were significantly improved, similar to those observed in the MCT + Sil group. These histological results indicated that rutaecarpine could inhibit fibrosis in MCT-induced PAH rats and confer protection to the pulmonary arteries.

To determine the mechanism of rutaecarpine in MCT-induced PAH, α-SMA-positive PASMCs were detected via immunohistochemical

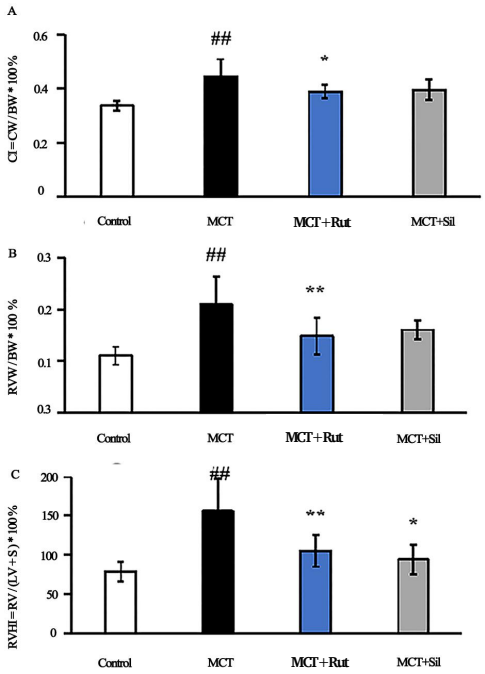

Figure 1 Effects of Rutaecarpine on CI, RVI and RVHI in PAH rats. (A) CI as the CW/BW ratio; (B) RVI as the RVW/BW ratio; (C) RVHI as the RV/LV + interventricular septum (S) ratio, four weeks after MCT injection. A mean ± SEM is used to present the result values. $^{\#\#}P < 0.01$ versus the control group, $^{*}P < 0.05$ versus the MCT group, $^{**}P < 0.01$ versus the MCT group. CI, cardiac index; CW, cardiac weight; BW, body weight; RV, right ventricle; RVI, right ventricle index; RVW, right ventricle weight; RVHI, right ventricle hypertrophy index; LV, left ventricle; MCT, monocrotaline; SEM, standard error of the mean.

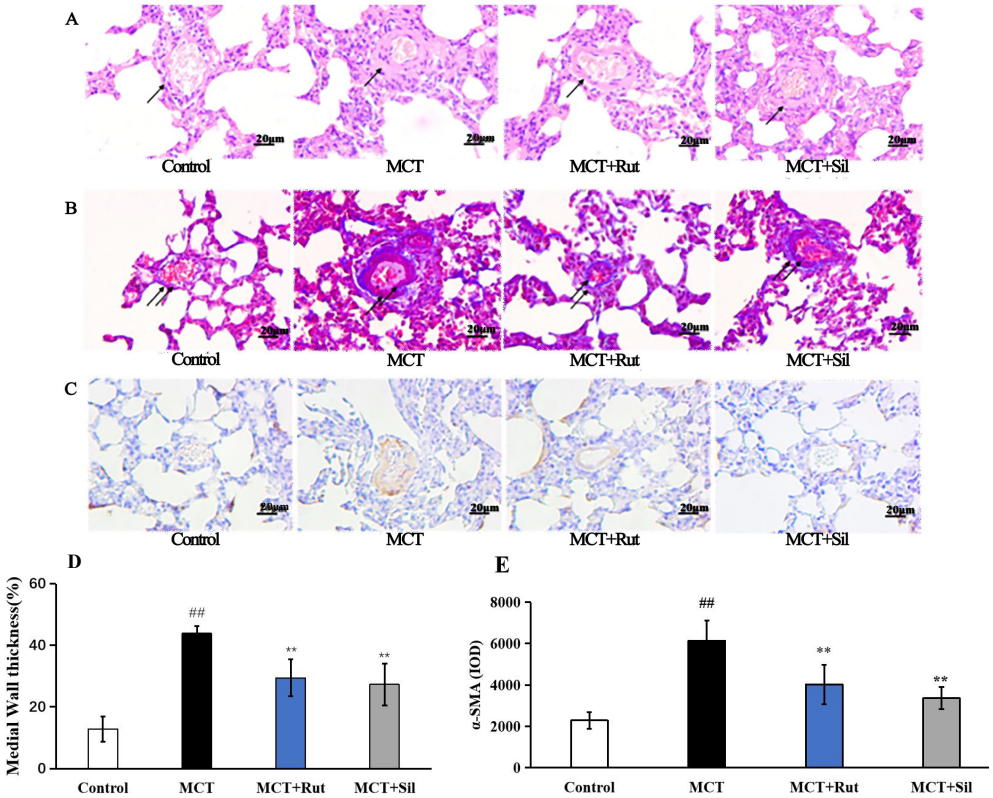

Figure 2 Rutaecarpine partially reverses the pathological remodeling of pulmonary artery hypertrophy. (A) Hematoxylin and eosin staining, 200×; (B) Masson staining, 200×; (C) immunohistochemical staining, 200×; (D) represents the percentage of medial wall thickness in pulmonary arteries; (E) represents the expression of α-SMA in pulmonary arteries. A mean ± SEM is used to present the result values. $^{\#\#}P < 0.01$ versus the control group, $^{*}P < 0.05$ versus the MCT group, $^{**}P < 0.01$ versus the MCT group. α-SMA, alpha-smooth muscle actin; SEM, standard error of the mean; MCT, monocrotaline.

staining. After administering MCT, the abundance of α-SMA-positive PASMCs increased (Figure 2C) and α-SMA expression increased 2.68-fold, compared to those in the control group ($P < 0.01$, Figure 2E). Quantitative analysis of α-SMA expression levels in the MCT + Rut and MCT + Sil groups showed significant improvements compared to that in the MCT group ($P < 0.01$).

H&E staining results of the right ventricular tissue showed that cardiomyocytes in the control group had appreciable continuity and regular arrangement with small gaps (Figure 3). Concurrently, the cardiomyocytes of rats injected with MCT showed marked proliferation and hypertrophy, disordered arrangement, sparseness and swelling cytoplasm. Additionally, rats treated with rutaecarpine and sildenafil exhibited significant histological improvement.

Rutaecarpine alleviates oxidative stress and inflammatory response

The effect of oxidative stress on pulmonary hypertension was investigated by monitoring changes in antioxidant and lipid peroxidation levels. MCT exposure resulted in increased lipid peroxidation MDA levels (Figure 4A–Figure 4C). Contrastingly, SOD and GSH-Px levels, generally associated with anti-oxidative stress responses, decreased 0.59- and 0.78-fold, compared to those in the control group ($P < 0.01$). Rats in the MCT + Rut group significantly showed improvement in these oxidative stress responses and the MCT + Sil group exhibited similar results, indicating that rutaecarpine antioxidant activity was involved in the reversal of PAH.

Inflammation in the pulmonary arteries was then evaluated to assess the anti-inflammatory effect of rutaecarpine. MCT treatment significantly upregulated proinflammatory cytokine levels, such as TNF-α, IL-1β and IL-6, compared to the control group (Figure 4D). Contrastingly, rats in the MCT + Rut and MCT + Sil groups showed effective reversal of the TNF-α ($P < 0.01$), IL-1β ($P < 0.05$) and IL-6 ($P < 0.01$) levels, demonstrating that anti-inflammatory activity contributed to the reversal of MCT-induced PAH.

Rutaecarpine alleviates PAH, inhibits proliferation and promotes apoptosis

The levels of p-ERK1/2, NF-κB p65 and ET-1 in the lungs of MCT-PAH rats were significantly increased by 1.43-, 2.10- and 1.95-fold, comparing the control and experimental groups. Meanwhile, the levels of p-ERK1/2, NF-κB p65 and ET-1 were significantly decreased in the MCT + Rut and MCT + Sil groups ($P < 0.05$, Figure 5), demonstrating that rutaecarpine exerted an anti-proliferative effect in MCT-PAH rats, which alleviated PAH.

Additionally, Bax, Bcl-2 and caspase-3 expression levels were detected by Western blot analysis to assess the impact of rutaecarpine on apoptosis. As shown in Figure 6, Bax expression was significantly reduced to 0.48 times that of the control group ($P < 0.05$), whereas Bcl-2 was significantly overexpressed (2.14 times; $P < 0.01$). However, these effects could be reversed in the MCT + Rut group

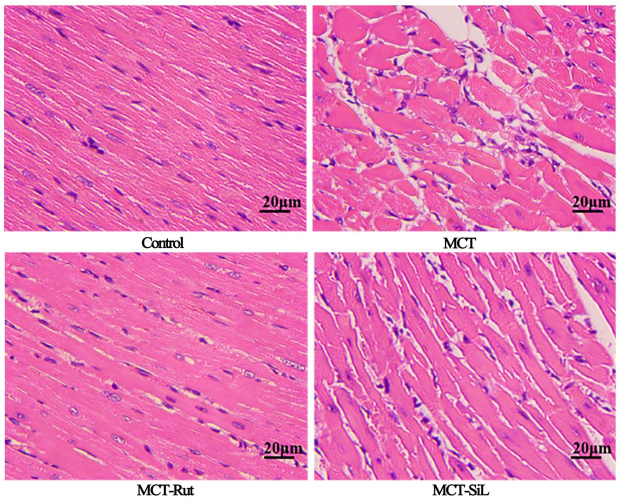

Figure 3 Rutaecarpine partially reverses the pathological remodeling of the right ventricle. hematoxylin and eosin, ×200. RV, right ventricle; MCT, monocrotaline.

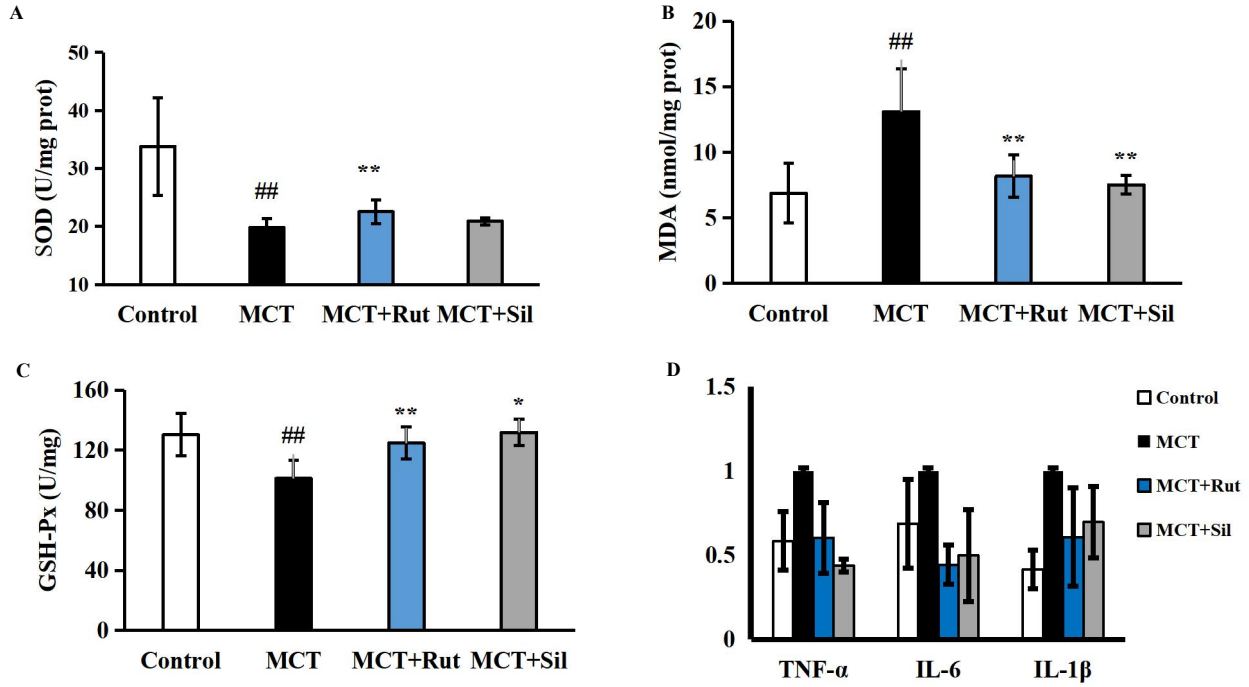

Figure 4 Rutaecarpine partially improves the changes in oxidative stress and inflammation in MCT-induced PAH rats. (A–C) SOD, MDA and GSH-Px were tested with their corresponding kits; (D) RT-qPCR analysis of relative TNF-α, IL-1β and IL-6 mRNA levels in peritoneal resident macrophages. A mean ± SEM is used to present the result values. $^{\#\#}P < 0.01$ versus the control group, $^{*}P < 0.05$ versus the MCT group, $^{**}P < 0.01$ versus the MCT group. MCT, monocrotaline; PAH, pulmonary arterial hypertension; SOD, superoxide dismutase; MDA, malondialdehyde; GSH-Px, glutathione peroxidase; RT-qPCR, reverse transcription-quantitative polymerase chain reaction; TNF-α, tumor necrosis factor-α; IL-1β, interleukin-1β; IL-6, interleukin-6.

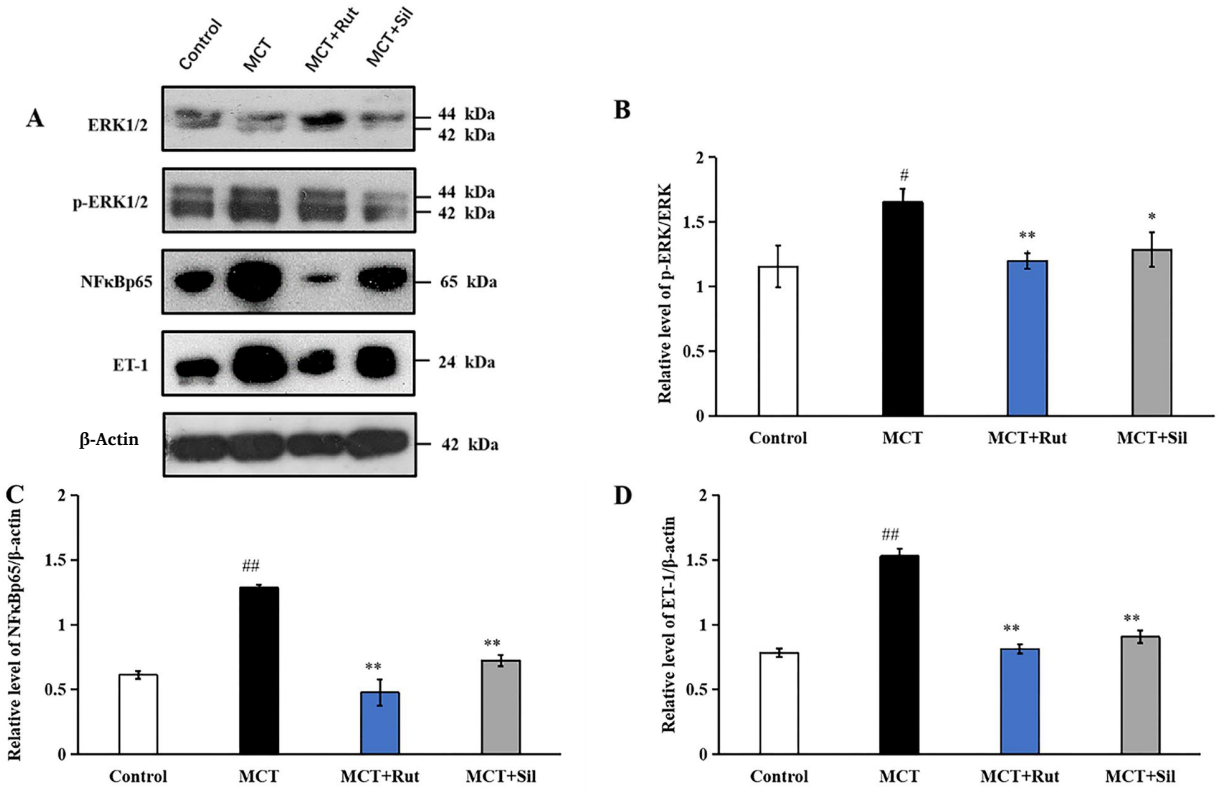

Figure 5 Effect of rutaecarpine on the protein expression of ERK1/2, p-ERK1/2, NK-κB p65, ET-1 shown by western blot. Normalization of expression levels was performed using β-actin. A mean ± SEM is used to present the result values. $^{\#\#}P < 0.01$ versus the control group, $^{*}P < 0.05$ versus the MCT group, $^{**}P < 0.01$ versus the MCT group. MCT, monocrotaline; ERK1/2, extracellular signal-regulated kinases 1/2; p-ERK1/2, phospho-extracellular signal-regulated kinases 1/2; NF-κB, nuclear factor kappa-B; ET-1, endothelin-1; SEM, standard error of the mean.

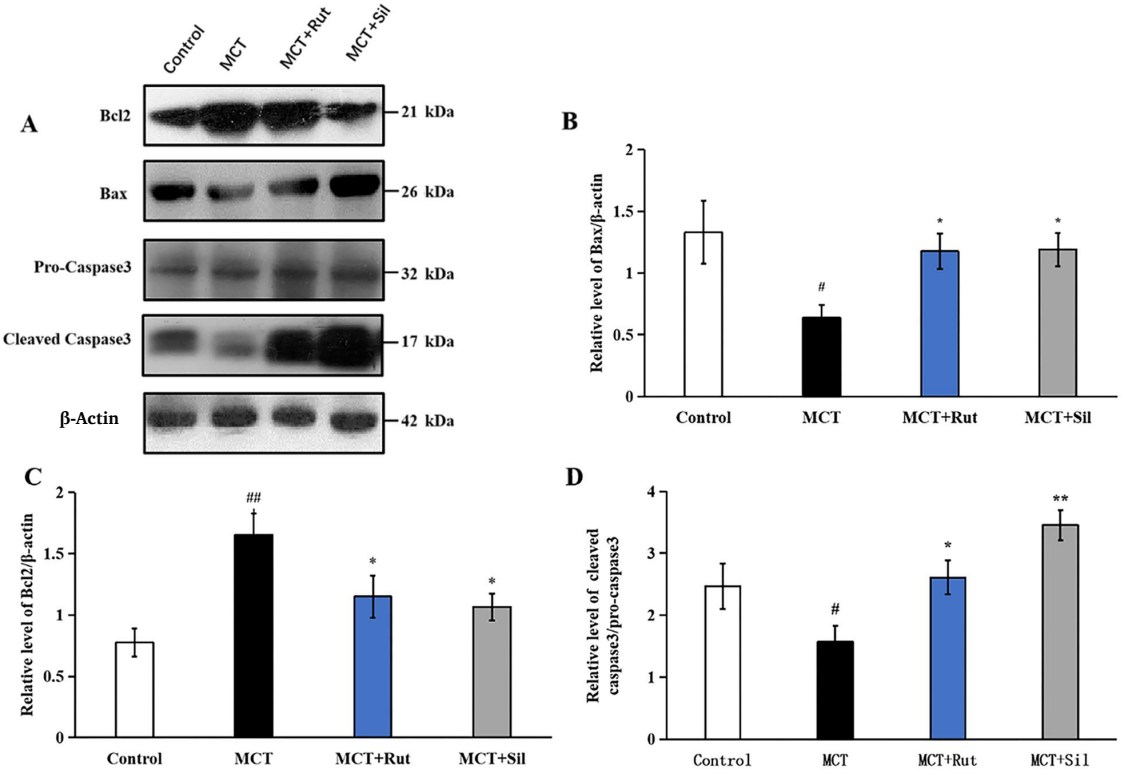

Figure 6 Effect of rutaecarpine on the protein expression of Bcl-2, Bax and pro-caspase-3 as determined by western blot analysis. Normalization of expression levels was performed using β-actin. A mean ± SEM is used to present the result values. $^{\#\#}P < 0.01$ versus the control group, $^{*}P < 0.05$ versus the MCT group, $^{**}P < 0.01$ versus the MCT group. Bcl-2, B cell lymphoma-2; SEM, standard error of the mean; MCT, monocrotaline.

(Figure 6A–Figure 6C; $P < 0.05$), similar to that in the MCT + Sil group. Therefore, MCT downregulated the relative levels of Bax/Bcl-2, whereas rutaecarpine treatment increased the Bax/Bcl-2 expression ratio. Finally, we detected the expression of cleaved caspase-3. As shown in Figure 6A and Figure 6D, cleaved caspase-3 level decreased to 0.64 times, compared with the control group ($P < 0.05$) and increased again under rutaecarpine and sildenafil treatments ($P < 0.05$).

Rutaecarpine inhibits autophagy

The impact of rutaecarpine therapy in autophagy was assessed via the expression of Beclin1, LC3-I, LC3-II and p62. As shown in Figure 7, MCT-PAH rats exhibited higher Beclin1 expression levels (2.26 times higher; $P < 0.01$) than the control group rats. Following treatment with rutaecarpine or sildenafil, the expression of Beclin1 reduced to 1.48 or 1.94 times that in the control group ($P < 0.01$ for MCT + Rut and $P < 0.05$ for MCT + Sil compared to the MCT group). Similarly, the LC3-II/β-actin ratio of MCT-PAH rats was increased by 3.36 times that in the control group ($P < 0.01$). After administration of rutaecarpine or sildenafil, the LC3-II/β-actin ratio significantly decreased compared to that in MCT-treated rats (by 1.18 and 1.48 times that of the control group respectively; $P < 0.01$). p62 is a central regulator of the autophagy process. The expression of p62 was reduced to 0.58 times in MCT-PAH rats when compared to control group ($P < 0.01$). Following treatment with rutaecarpine and sildenafil, the expression of p62 increased by 0.85-fold ($P < 0.05$).

Discussion

Our investigation in this study focused on the role and mechanism of rutaecarpine for PAH in a rat model. MCT-induced PAH in Sprague-Dawley rats was selected to test the efficacy of rutaecarpine in disease recovery. The effect was similar to that on human PAH in terms of hemodynamic and histopathological severity degree, including the upregulated expression of inflammatory cytokines, vascular remodeling, smooth muscle cell proliferation, endothelial dysfunction, and RV failure [27–29]. Moreover, sildenafil was selected as a positive control to comparatively validate the therapeutic effect of rutaecarpine, as it is considered an effective treatment for PAH [30]. This study demonstrated that rutaecarpine exhibited appreciable therapeutic effects in the MCT-induced PAH rat model, significantly reducing mPAP, RV index and RV hypertrophy index, and improving right ventricular hypertrophy. These results are similar with prior study, while the design in prior study absent positive control and the study focused on the dose of rutaecarpine (20 mg/kg versus 40 mg/kg) [31]. Additionally, in our study, the histological assessment of pathological sections showed that rutaecarpine treatment effectively counteracted pulmonary vascular wall thickening and restored lumen patency. The above-mentioned phenomena indicated that rutaecarpine played an important role in reversing pulmonary vascular and right ventricular remodeling in PAH.

The changes in pulmonary vascular wall thickening and expansion could affect the function of adjacent airways and lung parenchyma in PAH, causing abnormal changes in pulmonary function. Studies have reported that the vital capacity, Tiffeneau–Pinelli index, and maximum expiratory flow at 50% of forced vital capacity in PAH patients are significantly reduced, along with a decrease in the carbon monoxide diffusing capacity [32, 33]. 20–40% of patients with idiopathic pulmonary arterial hypertension have a significant decrease in forced expiratory volume in one second and forced expiratory volume in one second/forced vital capacity ratios (< 70%), indicating obstruction of the airways. Three quarters of idiopathic pulmonary arterial hypertension patients will have gas exchange impairment with a mean value of 59–71% of predicted values across earlier studies [34]. Our study reported similar results and indicated that the use of rutaecarpine could improve pulmonary function, including increased airway resistance and decreased lung compliance caused by PAH, but only pulmonary ventilation function was tested, but gas exchange function was not tested. Relevant studies on ventilation function will be carried out in future experiments.

IL-1, IL-6 and TNF-α, stimulate the expression of a variety of inflammatory factors, were frequently elevated in serum of patients and experimental PAH models and promote vascular remodeling [6]. In addition, TNF-α, IL-1β and IL-6 were associated with fibroblast proliferation and myofibroblast activation and that may improve with subjection to steroids or immunosuppressive therapy [6, 35–42]. We also observed an increase in TNF-α, IL-1β and IL-6 in the lungs of PAH rats. Compared with MCT group, collagen fiber proliferation and

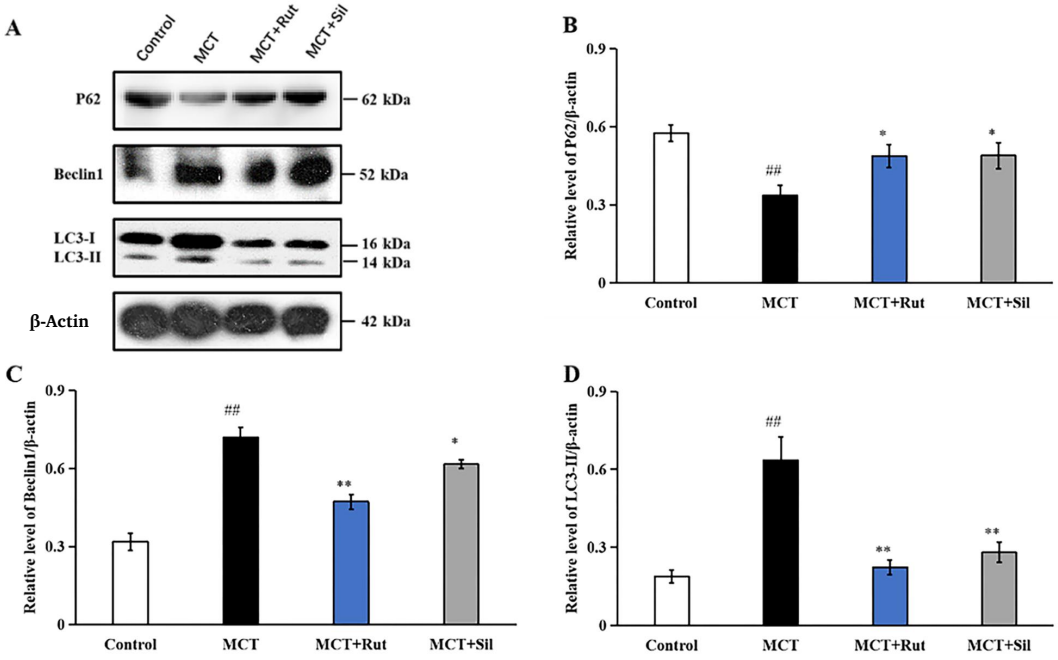

Figure 7 Effect of rutaecarpine on the protein expression of p62, Beclin1, LC3-I and LC3-II were determined using western blots. Normalization of expression levels was performed using β-actin. A mean ± SEM is used to present the result values. $^{\#\#}P < 0.01$ versus the control group, $^{*}P < 0.05$ versus the MCT group, $^{**}P < 0.01$ versus the MCT group. LC3, microtubule- associated protein light chain 3; SEM, standard error of the mean; MCT, monocrotaline.

inflammatory cell infiltration were significantly reduced in MCT + Rut group, similar to MCT + Sil group. Meanwhile, TNF-α, IL-6 and IL-1β levels were significantly downregulated in the MCT + Rut group, suggesting that rutaecarpine could alleviate PAH by inhibiting inflammatory responses.

There is a strong correlation between inflammation and oxidative stress. Studies have already reported that endothelial cell dysfunction and oxidative stress are involved in pulmonary vascular remodeling, and that the endogenous antioxidant defense system (including SOD and GSH) showed altered activity [43–45]. As the first line of defense against free radicals, oxidative enzyme systems such as SOD and GSH-Px play a crucial role, while MDA is generally believed to indicate oxidative damage. Oxidative stress leads to lipid peroxidation and leads to the production of substantial amounts of MDA, resulting in oxidative damage to PAECs. Evidence has increasingly demonstrated that oxidative stress contributes to PAH, thereby serving as a prognostic indicator[9, 46–49]. The results of our study suggested that rutaecarpine could be considered as a potential antioxidant therapeutic agent for PAH.

The activation of ERK1/2 and NF-κB promote the expression of ET-1, thereby promoting the proliferation of pulmonary smooth muscle cells and accelerating the development of pulmonary hypertension. ERK1/2 is a major member of the intracellular mitogen-activated protein kinase (MAPK) signaling pathway, which plays an important role in angiogenesis [50, 51]. The activation of ERK1/2 can enhance the expression of ET-1. Besides, when NF-κB is inactivated, it forms a complex with IκB, which is then distributed in the cytoplasm. IκB kinase is activated by the MAPK signaling pathway. After IκB kinase activation, IκB is phosphorylated, leading to IκB depolymerization and degradation through the ubiquitination-proteasome pathway. The p65 subunit of NF-κB is present in its free form in the cytoplasm following depolymerization and separation from IκB. Free NF-κB p65 is translocated to the nucleus, where it regulates the expression of target genes [52]. Independent in vivo and in vitro studies showed that smoking, low-density lipoprotein and hypertension could upregulate the expression of endothelin receptors in vascular smooth muscle cells through activation of the MAPK/NF-κB signaling pathway [53–55]. ET-1 is the strongest known endogenous angiotensin, causing marked pulmonary artery contraction and promoting the proliferation of vascular smooth muscle and fibrous tissue, which ultimately leads to increased pulmonary vascular resistance and pulmonary vascular remodeling [56–58]. This study demonstrated that rutaecarpine could inhibit proliferation and alleviate MCT-induced PAH by downregulating the expression of ERK1/2, nuclear NF-κB p65 and ET-1. Therefore, the current results suggest that rutaecarpine may improve pulmonary vascular remodeling.

Apoptosis resistance is also important for pulmonary smooth muscle cell proliferation [59]. In regulating apoptosis, the Bcl-2 protein family plays a key role. Apoptosis is controlled by both Bcl-2 and Bax; Bcl-2 inhibits it, whereas Bax promotes it [60]. Bcl-2, a pro-apoptotic protein, with exogenous or endogenous stimulating factors, can open the mitochondrial permeability transition pore; Apaf-1 and pro-caspase-9 form the apoptosome when cytochrome c interacts with them, which activates the caspase cascade to induce cell death [60]. In the present study, we noted that expression of the anti-apoptotic gene Bcl-2 was significantly upregulated in rats injected with MCT, whereas inhibited Bax and caspase-3. Rutaecarpine treatment decreased Bcl-2 expression levels and increased cleaved caspase-3 and Bax levels. These observations were in agreement with the previously reported findings on the changes in Bcl-2 levels and the anti-apoptotic effect of rutaecarpine in the treatment of cerebral ischemia-reperfusion injury, psoriasis, shock and other diseases [14, 17, 18, 58, 61]. Apoptotic resistance was significantly associated with the progression of PAH and rutaecarpine could treat PAH by regulating cell proliferation and apoptosis.

Autophagy is generally initiated in response to various stimuli, such as starvation, oxidative damage and chemical damage. Nonetheless, autophagy occurs at the basal level in most tissues to control the quality of organelles, but excessive activation is deleterious [62]. Recent studies have reported that autophagy is an important regulator of PAH pathogenesis [63–65]. Guo et al. demonstrated that Western blot analysis showed LC3B conversion increased and p62 expression decreased in in rats exposed to MCT [19]. Additionally, the activation of autophagy is associated with right ventricular failure in PAH mice [66]. In this study, autophagy was activated in PAH rats induced with MCT; the rats exhibited a significant increase in Beclin1 protein levels and LC3-II/LC3-I ratio, as well as a decrease in p62 protein levels. Meanwhile, rutaecarpine effectively inhibited autophagy, thereby reversing pulmonary hypertension.

Although the SOD activity assessed by reactive oxygen species and the drug works assessed by nitric oxide-cyclic guanosine phosphate were not assessed. The results of this study showed that rutaecarpine attenuated MCT-induced PAH by inhibiting inflammation, oxidative stress, proliferation and autophagy, as well as by promoting apoptosis. Therefore, rutaecarpine could be considered a novel therapeutic agent for PAH and further investigations should be performed to assess the potential connections among oxidative stress and the ERK1/2, nuclear NF-κB p65 and ET-1 pathways.

There are some limitations in this study. First of all, pulmonary hypertension patients are often accompanied by diffusion dysfunction. Pulmonary function test in this study did not detect diffusion function, which should be supplemented in future work. Second, the current study is limited to animal models and has not been validated at the cellular level, nor has it been applied to patients with pulmonary hypertension.

References

1. Hu B, Xu GT, Jin X, et al. Novel prognostic predictor for primary pulmonary hypertension: focus on blood urea nitrogen. *Front Cardiovasc Med*. 2021;8:724179. https://doi.org/10.3389/fcvm.2021.724179
2. Benza RL, Miller DP, Barst RJ, Badesch DB, Frost AE, McGoon MD. An evaluation of long-term survival from time of diagnosis in pulmonary arterial hypertension from the REVEAL Registry. *Chest*. 2012;142(2):448–456. https://doi.org/10.1378/chest.11-1460
3. Lajoie AC, Lauzière G, Lega JC, et al. Combination therapy versus monotherapy for pulmonary arterial hypertension: a meta-analysis. *Lancet Respir Med*. 2016;4(4):291–305. https://doi.org/10.1016/S2213-2600(16)00027-8
4. Liu X, Zhang SY, Wang XL, et al. Endothelial cell-derived SO_2 controls endothelial cell inflammation, smooth muscle cell proliferation, and collagen synthesis to inhibit hypoxic pulmonary vascular remodelling. *Oxid Med Cell Longev*. 2021; 2021:5577634. https://doi.org/10.1155/2021/5577634
5. Zhao Q, Song P, Zou MH. AMPK and pulmonary hypertension: crossroads between vasoconstriction and vascular remodeling. *Front Cell Dev Biol*. 2021;9:691585. https://doi.org/10.3389/fcell.2021.691585
6. Rabinovitch M, Guignabert C, Humbert M, Nicolls MR. Inflammation and immunity in the pathogenesis of pulmonary arterial hypertension. *Circ Res*. 2014;115(1):165–75. https://doi.org/10.1161/CIRCRESAHA.113.301141
7. Vaillancourt M, Ruffenach G, Meloche J, Bonnet S. Adaptation and remodelling of the pulmonary circulation in pulmonary hypertension. *Can J Cardiol*. 2015;31(4):407–415. https://doi.org/10.1016/j.cjca.2014.10.023
8. Freund-Michel V, Cardoso Dos Santos M, Guignabert C, et al. Role of nerve growth factor in development and persistence of experimental pulmonary hypertension. *Am J Respir Crit Care Med*. 2015;192(3):342–55. https://doi.org/10.1164/rccm.201410-1851OC
9. Jin HF, Liu MC, Zhang X, et al. Grape seed procyanidin extract attenuates hypoxic pulmonary hypertension by inhibiting oxidative stress and pulmonary arterial smooth muscle cells

proliferation. *J Nutr Biochem*. 2016;36:81–88. https://doi.org/10.1016/j.jnutbio.2016.07.006
10. Son JK, Chang HW, Jahng Y. Progress in studies on rutaecarpine. II. – synthesis and structure-biological activity relationships. *Molecules.* 2015;20(6):10800–10821. https://doi.org/10.3390/molecules200610800
11. Zhang YB, Yan TT, Sun DX, et al. Rutaecarpine inhibits KEAP1-NRF2 interaction to activate NRF2 and ameliorate dextran sulfate sodium-induced colitis. *Free Radic Biol Med*. 2020;148:33–41. https://doi.org/10.1016/j.freeradbiomed.2019.12.012
12. Luo JQ, Wang X, Jiang XH, et al. Rutaecarpine derivative R3 attenuates atherosclerosis via inhibiting NLRP3 inflammasome-related inflammation and modulating cholesterol transport. *FASEB J*. 2020;34(1):1398–1411. https://doi.org/10.1096/fj.201900903RRR
13. Arunachalam K, Damazo AS, Pavan E, et al. *Cochlospermum regium* (Mart. ex Schrank) Pilg.: evaluation of chemical profile, gastroprotective activity and mechanism of action of hydroethanolic extract of its xylopodium in acute and chronic experimental models. *J Ethnopharmacol*. 2019;233:101–114. https://doi.org/10.1016/j.jep.2019.01.002
14. Han MY, Hu L, Chen Y. Rutaecarpine may improve neuronal injury, inhibits apoptosis, inflammation and oxidative stress by regulating the expression of ERK1/2 and Nrf2/HO-1 pathway in rats with cerebral ischemia-reperfusion injury. *Drug Des Devel Ther*. 2019;13:2923–2931. https://doi.org/10.2147/DDDT.S216156
15. Li WQ, Li XH, Du J, et al. Rutaecarpine attenuates hypoxia-induced right ventricular remodeling in rats. *Naunyn Schmiedebergs Arch Pharmacol*. 2016;389(7):757–767. https://doi.org/10.1007/s00210-016-1240-8
16. Jin SW, Hwang YP, Choi CY, et al. Protective effect of rutaecarpine against t-BHP-induced hepatotoxicity by upregulating antioxidant enzymes via the CaMKII-Akt and Nrf2/ARE pathways. *Food Chem Toxicol*. 2017;100:138–148. https://doi.org/10.1016/j.fct.2016.12.031
17. Li YJ, Zhang GY, Chen ML, et al. Rutaecarpine inhibited imiquimod-induced psoriasis-like dermatitis via inhibiting the NF-κB and TLR7 pathways in mice. *Biomed Pharmacother*. 2019;109:1876–1883. https://doi.org/10.1016/j.biopha.2018.10.062
18. Li ZL, Yang MS, Peng Y, Gao M, Yang BC. Rutaecarpine ameliorated sepsis-induced peritoneal resident macrophages apoptosis and inflammation responses. *Life Sci*. 2019;228:11–20. https://doi.org/10.1016/j.lfs.2019.01.038
19. Guo LY, Li YB, Tian Y, et al. eIF2α promotes vascular remodeling via autophagy in monocrotaline-induced pulmonary arterial hypertension rats. *Drug Des Devel Ther*. 2019;13:2799–2809. https://doi.org/10.2147/DDDT.S213817
20. Zeng SY, Yang L, Lu HQ, Yan QJ, Gao L, Qin XP. Rutaecarpine prevents hypertensive cardiac hypertrophy involving the inhibition of Nox4-ROS-ADAM17 pathway. *J Cell Mol Med*. 2019;23(6):4196–4207. https://doi.org/10.1111/jcmm.14308
21. Bae HK, Lee H, Kim KC, Hong YM. The effect of sildenafil on right ventricular remodeling in a rat model of monocrotaline-induced right ventricular failure. *Korean J Pediatr*. 2016;59(6):262–270. https://doi.org/10.3345/kjp.2016.59.6.262
22. Xu DQ, Li Y, Zhang B, et al. Resveratrol alleviate hypoxic pulmonary hypertension via anti-inflammation and anti-oxidant pathways in rats. *Int J Med Sci*. 2016;13(12):942–954. https://doi.org/10.7150/ijms.16810
23. Ren ZX, Li JS, Shen JL, et al. Therapeutic sildenafil inhibits pulmonary damage induced by cigarette smoke exposure and bacterial inhalation in rats. *Pharm Biol*. 2020;58(1):116–123. https://doi.org/10.1080/13880209.2019.1711135
24. He YZ, Cao XP, Liu XS, et al. Quercetin reverses experimental pulmonary arterial hypertension by modulating the TrkA pathway. *Exp Cell Res*. 2015;339(1):122–134. https://doi.org/10.1016/j.yexcr.2015.10.013
25. Zhao TF, Wang SY, Zou XZ, Zhao HD. MiR-593-5p promotes the development of hypoxic-induced pulmonary hypertension via targeting PLK1. *Eur Rev Med Pharmacol Sci*. 2019;23(8):3495–3502. https://doi.org/10.26355/eurrev_201904_17715
26. Bakan N, Taysi S, Yilmaz O, et al. Glutathione peroxidase, glutathione reductase, Cu-Zn superoxide dismutase activities, glutathione, nitric oxide, and malondialdehyde concentrations in serum of patients with chronic lymphocytic leukemia. *Clin Chim Acta*. 2003;338(1-2):143–149. https://doi.org/10.1016/j.cccn.2003.08.013
27. Polonio IB, Acencio MM, Pazetti R, et al. Lodenafil treatment in the monocrotaline model of pulmonary hypertension in rats. *J Bras Pneumol*. 2014;40(4):421–424. https://doi.org/10.1590/S1806-37132014000400010
28. Medoff BD, Okamoto Y, Leyton P, et al. Adiponectin deficiency increases allergic airway inflammation and pulmonary vascular remodeling. *Am J Respir Cell Mol Biol.* 2009;41(4):397–406. https://doi.org/10.1165/rcmb.2008-0415OC
29. Fuji S, Matsushita S, Hyodo K, et al. Association between endothelial function and micro-vascular remodeling measured by synchrotron radiation pulmonary micro-angiography in pulmonary arterial hypertension. *Gen Thorac Cardiovasc Surg*. 2016;64(10):597–603. https://doi.org/10.1007/s11748-016-0684-6
30. Vizza CD, Sastry BK, Safdar Z, et al. Efficacy of 1, 5, and 20 mg oral sildenafil in the treatment of adults with pulmonary arterial hypertension: a randomized, double-blind study with open-label extension. *BMC Pulm Med*. 2017;17(1):44. https://doi.org/10.1186/s12890-017-0374-x
31. Li XW, Wang XM, Li S, Yang JR. Effects of rutaecarpine on right ventriclar remodeling in rats with monocrotaline-induced pulmonary hypertension. *Chin J Appl Physiol*. 2014;30(5):405–410. (Chinese) https://doi.org/10.13459/j.cnki.cjap.2014.05.006
32. Farkhooy A, Bellocchia M, Hedenström H, et al. Lung function in relation to six-minute walk test in pulmonary hypertension. *Eur Clin Respir J*. 2020;7(1):1745492. https://doi.org/10.1080/20018525.2020.1745492
33. Hajsadeghi S, Mirshafiee S, Pazoki M, et al. The relationship between global longitudinal strain and pulmonary function tests in patients with scleroderma and normal ejection fraction and pulmonary artery pressure: a case-control study. *Int J Cardiovasc Imaging*. 2020;36(5):883–888. https://doi.org/10.1007/s10554-020-01788-7
34. Low AT, Medford AR, Millar AB, Tulloh RM. Lung function in pulmonary hypertension. *Respir Med*. 2015;109(10):1244–1249. https://doi.org/10.1016/j.rmed.2015.05.022
35. Meléndez GC, McLarty JL, Levick SP, Du Y, Janicki JS, Brower GL. Interleukin 6 mediates myocardial fibrosis, concentric hypertrophy, and diastolic dysfunction in rats. *Hypertension*. 2010;56(2):225–231. https://doi.org/10.1161/HYPERTENSIONAHA.109.148635
36. Pellman J, Zhang J, Sheikh F. Myocyte-fibroblast communication in cardiac fibrosis and arrhythmias: mechanisms and model systems. *J Mol Cell Cardiol*. 2016;94:22–31. https://doi.org/10.1016/j.yjmcc.2016.03.005
37. Huang ZW, Liu ZH, Luo Q, et al. Glycoprotein 130 inhibitor ameliorates monocrotaline-induced pulmonary hypertension in rats. *Can J Cardiol*. 2016;32(11):1356.e1-1356.e10. https://doi.org/10.1016/j.cjca.2016.02.058
38. Soon E, Crosby A, Southwood M, et al. Bone morphogenetic protein receptor type II deficiency and increased inflammatory cytokine production. A gateway to pulmonary arterial hypertension. *Am J Respir Crit Care Med*. 2015;192(7):859–872.

https://doi.org/10.1164/rccm.201408-1509OC
39. Fujita M, Mason RJ, Cool C, Shannon JM, Hara N, Fagan KA. Pulmonary hypertension in TNF-alpha-overexpressing mice is associated with decreased VEGF gene expression. *J Appl Physiol* (1985). 2002;93(6):2162–2170. https://doi.org/10.1152/japplphysiol.00083.2002
40. Birnhuber A, Crnkovic S, Biasin V, et al. IL-1 receptor blockade skews inflammation towards Th2 in a mouse model of systemic sclerosis. *Eur Respir J*. 2019;54(3):1900154. https://doi.org/10.1183/13993003.00154-2019
41. Durham GA, Palmer TM. Is there a role for prostanoid-mediated inhibition of IL-6 trans-signalling in the management of pulmonary arterial hypertension. *Biochem Soc Trans*. 2019; 47(4):1143–1156. https://doi.org/10.1042/BST20190046
42. Becker MO, Radic M, Schmidt K, et al. Serum cytokines and their predictive value in pulmonary involvement of systemic sclerosis. *Sarcoidosis Vasc Diffuse Lung Dis*. 2019;36(4):274–284. https://doi.org/10.36141/svdld.v36i4.7612
43. Archer S, Rich S. Primary pulmonary hypertension: a vascular biology and translational research “work in progress”. *Circulation*. 2000;102(22):2781–2791. https://doi.org/10.1161/01.CIR.102.22.2781
44. Karuppiah K, Druhan LJ, Chen CA, et al. Suppression of eNOS-derived superoxide by caveolin-1: a biopterin-dependent mechanism. *Am J Physiol Heart Circ Physiol*. 2011;301(3): H903–H911. https://doi.org/10.1152/ajpheart.00936.2010
45. Fu CP, Hao SY, Liu ZL, et al. SOD2 ameliorates pulmonary hypertension in a murine model of sleep apnea via suppressing expression of NLRP3 in $CD11b^+$ cells. *Respir Res*. 2020;21(1):9. https://doi.org/10.1186/s12931-019-1270-0
46. Rawat DK, Alzoubi A, Gupte R, et al. Increased reactive oxygen species, metabolic maladaptation, and autophagy contribute to pulmonary arterial hypertension-induced ventricular hypertrophy and diastolic heart failure. *Hypertension*. 2014; 64(6):1266–1274. https://doi.org/10.1161/HYPERTENSIONAHA.114.03261
47. Iwata K, Ikami K, Matsuno K, et al. Deficiency of NOX1/nicotinamide adenine dinucleotide phosphate, reduced form oxidase leads to pulmonary vascular remodeling. *Arterioscler Thromb Vasc Biol*. 2014;34(1):110–119. https://doi.org/10.1161/ATVBAHA.113.302107
48. Aggarwal S, Gross CM, Sharma S, Fineman JR, Black SM. Reactive oxygen species in pulmonary vascular remodeling. *Compr Physiol*. 2013;3(3):1011–1034. https://doi.org/10.1002/cphy.c120024
49. Smukowska-Gorynia A, Rzymski P, Marcinkowska J, et al. Prognostic value of oxidative stress markers in patients with pulmonary arterial or chronic thromboembolic pulmonary hypertension. *Oxid Med Cell Longev*. 2019;2019:3795320. https://doi.org/10.1155/2019/3795320
50. Menon RT, Shrestha AK, Barrios R, Reynolds C, Shivanna B. Tie-2 cre-mediated deficiency of extracellular signal-regulated kinase 2 potentiates experimental bronchopulmonary dysplasia-associated pulmonary hypertension in neonatal mice. *Int J Mol Sci*. 2020;21(7):2408. https://doi.org/10.3390/ijms21072408
51. Song HJ, Kim JS, Lee MJ, Nam YS, Sohn UD. Reactive oxygen species mediate ET-1-induced activation of ERK1/2 signaling in cultured feline esophageal smooth muscle cells. *Arch Pharm Res*. 2007;30(9):1080–1087. https://doi.org/10.1007/BF02980241
52. Cheng BF, Gao YX, Lian JJ, et al. Anti-inflammatory effects of pitavastatin in interleukin-1β-induced SW982 human synovial cells. *Int Immunopharmacol*. 2017;50:224–229. https://doi.org/10.1016/j.intimp.2017.06.032
53. Zhang YP, Zhang W, Edvinsson L, Xu CB. Lipid-soluble cigarette smoke particles induced vascular endothelin type a receptor up-regulation through activation of ERK1/2 signal pathways. *Basic Clin Pharmacol Toxicol*. 2017;120(4):327–334. https://doi.org/10.1111/bcpt.12688
54. Liu Y, Chen XL, Xu CB, et al. Tail vein injection of mmLDL upregulates mouse mesenteric artery ET_B receptors via activation of the ERK1/2 pathway. *Vascul Pharmacol*. 2017; 96–98:33–39. https://doi.org/10.1016/j.vph.2017.08.002
55. Cao L, Cao YX, Xu CB, Edvinsson L. Altered endothelin receptor expression and affinity in spontaneously hypertensive rat cerebral and coronary arteries. *PLoS One*. 2013;8(9):e73761. https://doi.org/10.1371/journal.pone.0073761
56. Satwiko MG, Ikeda K, Nakayama K, et al. Targeted activation of endothelin-1 exacerbates hypoxia-induced pulmonary hypertension. *Biochem Biophys Res Commun*. 2015;465(3): 356–362. https://doi.org/10.1016/j.bbrc.2015.08.002
57. Ozen G, Benyahia C, Amgoud Y, et al. Interaction between PGI_2 and ET-1 pathways in vascular smooth muscle from Group-III pulmonary hypertension patients. *Prostaglandins Other Lipid Mediat*. 2020;146:106388. https://doi.org/10.1016/j.prostaglandins.2019.106388
58. Raish M, Ahmad A, Ansari MA, et al. Momordica charantia polysaccharides ameliorate oxidative stress, inflammation, and apoptosis in ethanol-induced gastritis in mucosa through NF-kB signaling pathway inhibition. *Int J Biol Macromol*. 2018;111: 193–199. https://doi.org/10.1016/j.ijbiomac.2018.01.008
59. Schermuly RT, Ghofrani HA, Wilkins MR, Grimminger F. Mechanisms of disease: pulmonary arterial hypertension. *Nat Rev Cardiol*. 2011;8(8):443–455. https://doi.org/10.1038/nrcardio.2011.87
60. Hassan M, Watari H, AbuAlmaaty A, Ohba Y, Sakuragi N. Apoptosis and molecular targeting therapy in cancer. *Biomed Res Int*. 2014;2014:150845. https://doi.org/10.1155/2014/150845
61. Xie L, Guo YL, Chen YR, et al. A potential drug combination of omeprazole and patchouli alcohol significantly normalizes oxidative stress and inflammatory responses against gastric ulcer in ethanol-induced rat model. *Int Immunopharmacol*. 2020; 85:106660. https://doi.org/10.1016/j.intimp.2020.106660
62. Liao SX, Sun PP, Gu YH, Rao XM, Zhang LY, Ou-Yang Y. Autophagy and pulmonary disease. *Ther Adv Respir Dis*. 2019; 13:1753466619890538. https://doi.org/10.1177/1753466619890538
63. Kato F, Sakao S, Takeuchi T, et al. Endothelial cell-related autophagic pathways in Sugen/hypoxia-exposed pulmonary arterial hypertensive rats. *Am J Physiol Lung Cell Mol Physiol*. 2017;313(5):L899–L915. https://doi.org/10.1152/ajplung.00527.2016
64. Racanelli AC, Kikkers SA, Choi AMK, Cloonan SM. Autophagy and inflammation in chronic respiratory disease. *Autophagy*. 2018;14(2):221–232. https://doi.org/10.1080/15548627.2017.1389823
65. Long L, Yang XD, Southwood M, et al. Chloroquine prevents progression of experimental pulmonary hypertension via inhibition of autophagy and lysosomal bone morphogenetic protein type II receptor degradation. *Circ Res*. 2013;112(8): 1159–1170. https://doi.org/10.1161/CIRCRESAHA.111.300483
66. Ibrahim YF, Shults NV, Rybka V, Suzuki YJ. Docetaxel Reverses Pulmonary Vascular Remodeling by Decreasing Autophagy and Resolves Right Ventricular Fibrosis. *J Pharmacol Exp Ther*. 2017; 363(1):20–34. https://doi.org/10.1124/jpet.117.239921